Lidar-based wake tracking for closed-loop wind farm control

Steffen Raach[1], David Schlipf[1], and Po Wen Cheng[1]

[1]Stuttgart Wind Energy (SWE), University of Stuttgart, Allmandring 5B, 70569 Stuttgart, Germany

Correspondence to: Steffen Raach (raach@ifb.uni-stuttgart.de)

Abstract. This work presents two advancements towards closed-loop wake redirecting of a wind turbine. First, a model-based wake tracking approach is presented which uses a nacelle-based lidar system facing downwind to obtain information about the wake. The method uses a reduced order wake model to track the wake. The tracking is demonstrated with lidar measurement data from an offshore campaign and with simulated lidar data from a SOWFA simulation. Second, a controller for closed-loop wake steering is presented. It uses the wake tracking information to set the yaw actuator of the wind turbine to redirect the wake to a desired position. Altogether, the two approaches enable a closed-loop wake redirection.

1 Introduction

In recent years, wind farm control has gained more and more importance in the wind energy control community, since wind turbines in a wind farm can interact by their flow. The interaction can result in less power compared to a fee-stream operation and can result in higher structural load of the downstream turbine due to higher turbulence in the flow and possible partial wake impingements. The wind speed in the wake of a wind turbine is reduced with respect to the free stream wind speed. Additionally, the turbulence in the wake is increased. If a wind turbine is hit by a wake from a wind turbine located upwind, the wind turbine produces less power and is faced with higher structural loads because of the increased turbulence, see Borisade et al. (2015). Describing the wake effects and quantifying the decay has been of interest for years. Different models have been developed to address different phenomena, such as the velocity deficit and the increased turbulence intensity. There are empirical models, data driven models, and models which describe the physical behavior in the wake, all varying in complexity and computational effort. Mainly, models with low complexity are steady state models which means they describe the interaction in a static manner and no wake propagation is modeled. Further research is needed to develop control oriented dynamic wake models.

The same two goals are valid for both wind turbine and wind farm control: 1) maximization of the total power and 2) reduction of the structural loads. Two main concepts has been introduced for wind farm control: 1) axial induction control and 2) wake redirection control. Axial induction control aims at manipulating the axial induction by the blade pitch or torque actuator and steering the wind turbine to a lower production level. This results in a weaker wake deficit and aims at minimizing structural load effects on the downwind wind turbines and preserving energy in the flow for downstream turbines. The effects on the overall energy capture of the wind farm is not clear yet. Consider Boersma et al. (2017) for a general overview on wind farm control.

The idea of redirecting the wake by the yaw actuator instead of trying to mitigate its intensity has been discussed in different publications, see Fleming et al. (2014b, a); Gebraad et al. (2014). In simulation studies it was shown that the wake is redirected up to 0.54 times the rotor diameter (at seven diameter downwind distance) by yawing the turbine up to $40\,\mathrm{deg}$. Different investigations have shown promising results in improving the power output of a wind farm by applying yaw offsets in open-loop approaches, see Gebraad et al. (2014) and Fleming et al. (2014a). Nevertheless, the form in which it has been applied so far does contain drawbacks: 1) Applying optimized yaw angles in a feed-forward approach does not guarantee that the wake is going to the desired direction - thus, the quality of the model, which is used to compute the yaw angles, highly influences the control performance. 2) There is no observation of whether the wake is being redirected correctly. The concept of closed-loop wake redirection, which was introduced in Raach et al. (2016), can help to overcome the drawbacks.

A major barrier for wind farm control applications has been the lack of measurement devices to measure the flow interactions between wind turbines, but also their cost and availability. Further, modeling the three dimensional flow field is not a straight forward approach since the flow is usually described by the Navier-Stokes equations. Lidar can be a useful tool to address the measurement problem in wind farm applications, while bearing in mind the instrument limitations and the assumptions required to extract the information and exploit the lidar measurement data.

This paper addresses the wind farm control concept of wake redirecting. It aims to enable closed-loop wake redirecting by presenting a method to obtain the wake position using lidar measurements. Further, the difficulty in wake position definition and measurability is discussed.

First, it presents a model-based estimation approach to obtain important quantities for wake redirecting using a nacelle-based lidar system facing downwind. Furthermore, a closed loop controller is designed and analyzed. In summary, this work presents an entire concept for lidar-based closed-loop wake redirecting.

2   Methodology

In order to enable a lidar-based closed-loop wake redirecting within a wind farm, the problem can be divided into two main tasks: 1) the measurement task and 2) the control task. This work focuses mainly on the measurement task but gives also a summary of a solution to the control task, which was presented in Raach et al. (2016). Figure 1 presents the general concept of the closed-loop wake redirecting and the link between measurement task and control task.

2.1   Problem formulation for wake-tracking

When talking about wake tracking or a wake center position a main problem exists. There is no clear definition of the wake center, moreover, the idea of a wake center is a concept based on time averaged profiles of the wake behind a turbine (1 to 10 minutes averages). Averaging the flow yields a (double) Gaussian function for the velocity deficit profile in the horizontal and vertical directions. From this a wake center can then be defined easily. However, when different methods are used to define the shape, wake center estimates may be vary under the same flow conditions, see Vollmer et al. (2016). The absence of a
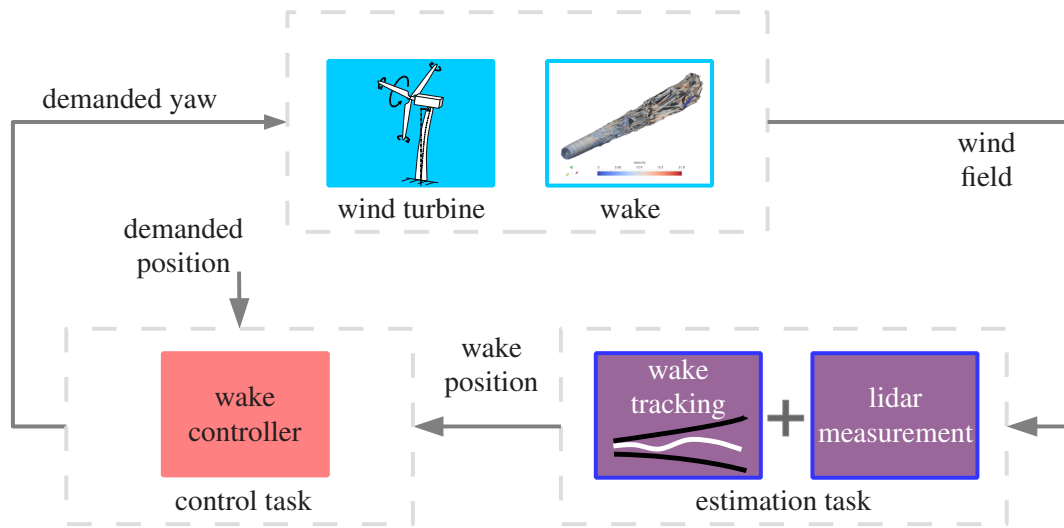
Figure 1. The conceptual idea of closed-loop wake redirecting and its two main tasks: 1) the estimation task addressed in Section 5 and 2) the control task addressed in Section 6.

unique wake center definition must be considered when comparing results. Furthermore, this means even with full flow field information the wake center is not a measurable quantity and depends on definition.

For lidar-based wake tracking, first, a reference definition of the wake center and is needed. Then, the result of the estimation method from the lidar measurement data can be compared to the reference definition.

2.2 The estimation task

Measuring flow quantities is crucial for enabling a closed-loop controller to manipulate the wake quantities. The task of the measurement problem is to provide the necessary quantities for the controller. This means using a measurement device, a lidar, and processing the measurement data in such a way that they are useful for the controller. Since the lidar measurement principle has several limitations in providing wind field information an adequate estimation technique is used that is described in Section 5.

2.3 The control task

The second task towards a closed-loop wake redirection is the control task. Its main challenge is to convert the estimated wake position information and the demanded position to a demanded yaw signal. A feedback controller has to be designed which steers the wake center to the desired position and compensates for uncertainties in the models. Since the reaction of a change

in the yaw is measured with a delay due to the wake propagation time, the controller has to be designed in such a way that it can overcome this limitation.

In the following, the measurement problem is addressed first. A method is presented to estimate wake information from lidar measurement data using a nacelle-based lidar system. Second, the controller problem is addressed in Section 6. A wake redirecting controller is presented which uses the obtained wake information, namely the wake center position, and steers the wake center using the yaw actuator to a desired position.

The overall goal of this paper is to also present the framework of lidar-based closed-loop wake redirection with exemplary models and controller.

3   Reference definition and its impact on the estimation task

3.1   Wake center definition

As previously mentioned, it is first necessary to define the wake center. The minimum wind power method proposed by Vollmer et al. (2016) is adopted and modified to identify the wake center. Thus, it is defined as the position where a second wind turbine, which orientated identically and has the same rotor diameter than the first, would produce the least power. This yields the minimization problem

$$\min_{y} \int\limits_{0}^{2\pi} \int\limits_{y}^{R+y} u(r,\phi)^3 r \, \mathrm{d}r\mathrm{d}\phi, \tag{1}$$

where the position of the turbine is described in the polar coordinate system (r,ϕ) with the origin at y and $z = 0$ (hub-height). The definition then assumes that the wake center is at (y,z).

The flow field is time averaged over different running window lengths and the impact of the wind lengths is analyzed. The calculated wake center filtered with a running averaged filter with different window lengths are presented in Figure 2. The presented results are for a low turbulence ($TI = 6\%$) SOWFA simulation under a mean hub-height free-stream wind speed $8\,\mathrm{ms}^{-1}$. The available flow field data has a sampling frequency of $1\,\mathrm{Hz}$ and the wake center is calculated from each sample. The wake center clearly converges to a steady value with increasing averaging time T.

3.2   Problem discussion of lidar-based wake tracking

Compared to other problems in lidar-based wind field reconstruction the problem of wake center estimation is different. Other model based approaches in wind field reconstruction (e.g. estimation of the rotor-effective wind speed, or of u and v wind vector components using lidar measurements as in Schlipf et al. (2012)) can first be compared to existing quantities. Further, the used models can be used to predict line-of-sight velocities (v_{los}) of lidar measurements and be directly compared to the real data. Therefore, the model can be used in two directions, estimating and predicting the wind field.
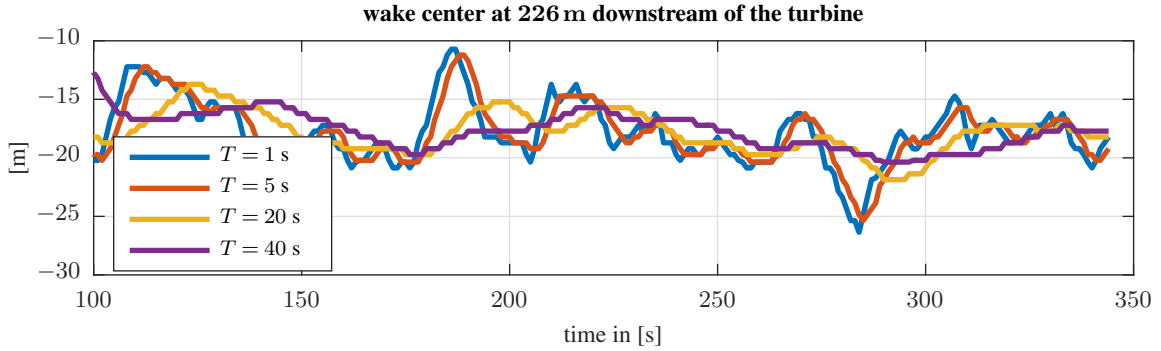
4

Figure 2. Time evolution of wake center when different window lengths T are used to average the flow during the wake center calculation.

Here, having the wake center defined like in Eq. (1) the prediction of the wind field from a given position is not possible and further a direct comparison of line-of-sight data is not possible. Nevertheless, the wake center position definition seems to be very convenient and is therefore used as reference.

4 A simplified wake model for wake tracking

5 The estimation task addresses the processing and estimation of useful information and provides them to the controller. Since a lidar system has several limitations, the desired quantities, like the wake position, or the wake deficit, are not measurable and have to be estimated from the measurement data. One main limitation of a lidar system is that it only returns the projection of the wind speeds along the direction of the laser beam. This means that a lidar system only provides scalar information of the actual wind vectors. Further, the wind speed is not measured at a certain point but in a volume around the desired measure-
10 ment location. A solution to this limitations is to implement model-based wind field reconstruction. Wind field reconstruction methods have been developed and used for different applications of lidar system usage in wind energy, for example static two- and three-dimensional, Schlipf et al. (2012), dynamic three dimensional wind field reconstruction methods, see Raach et al. (2014), and approaches for floating lidar systems, Schlipf et al. (2012). Here, the concept of wind field reconstruction is used to obtain information about the wake.
15 The general approach of wind field reconstruction from lidar data is to estimate wind field characteristics from an internal model by fitting simulated lidar data to the measured ones. In Figure 3 the basic idea of model-based wind field reconstruction is shown. An optimizer is used to find the best fit for a model of the assumed wind field with the defined lidar configuration. The optimizer minimizes the square error of the modeled (simulated) $v_{los,s}$ and the measured $v_{los,m}$ lidar line-of-sight velocities and returns the estimated model parameter (e.g. wake center position, wake decay, wake deficit, etc.).
20 In this work, a lidar and a wind field model is used. The wind field model consists of a background wind field model, which defines the ambient wind speed and its profile, and a wake model. The wake model includes the main wake effects: wake deficit, wake evolution, and wake center displacement. The models are presented in the following section.
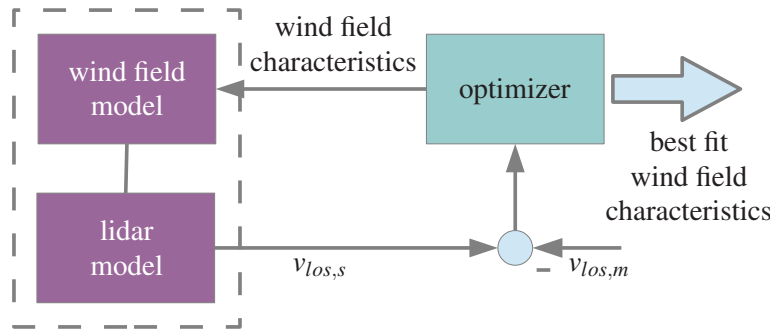
5

Figure 3. The general concept of model-based wind field reconstruction, in which the wind field characteristics are estimated by fitting simulated lidar measurement data ($v_{los,s}$) to measurements ($v_{los,m}$).

4.1 Wind field model

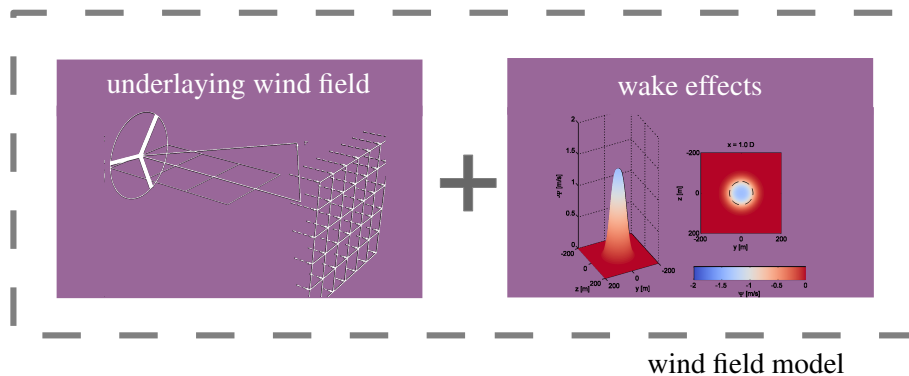Figure 4 shows the subparts of the wind field model: 1) the underlaying wind field, and 2) the wake model.

Figure 4. The submodels of the wind field model (in the wind coordinate system W): 1) the underlaying wind field, and 2) the wake model.

The wind field model is described in a wind coordinate system which is denoted by the subscript W. It is rotated horizontally with respect to the global inertial coordinate system I and aligned with the wind direction. The wind speed vector in the W-system is transformed in the I-system by

$$\begin{bmatrix} u \\ v \\ w \end{bmatrix}_I = \begin{bmatrix} \cos\alpha & -\sin\alpha & 0 \\ \sin\alpha & \cos\alpha & 0 \\ 0 & 0 & 1 \end{bmatrix} \begin{bmatrix} u \\ v \\ w \end{bmatrix}_W , \tag{2}$$

where α is the horizontal rotation of the wind field. The underlying wind field includes the rotor effective wind speed v_0 and vertical linear shear δ_V. It is assumed that the wind field has only a u component. Thus, in the W coordinate system, the

underlying wind field vector at point i with the coordinates $\left[x_i, y_i, z_i\right]^T$

$$\begin{bmatrix} u \\ v \\ w \end{bmatrix}_{i,W} = \begin{bmatrix} v_0 + z_i\delta_V \\ 0 \\ 0 \end{bmatrix},$$ (3)

where z_i is the height above the ground. This is illustrated in Figure 4 on the left. Further, the wind field is linearly overlaid with the wake model Ψ for the u and v components yielding

$$\begin{bmatrix} u \\ v \\ w \end{bmatrix}_{i,W} = \begin{bmatrix} v_0 + z_i\delta_V + \Psi_{u,i} \\ \Psi_{v,i} \\ 0 \end{bmatrix}.$$ (4)

In the following section, the considered wake effects are described and the wake model is presented.

4.1.1 Wake deficit and wake evolution model.

The rotor extracts energy from the wind and converts it into electrical energy. Therefore, the wind speed is reduced behind a wind turbine. Through mixing and energy flow from the surrounding the momentum deficit recovers. The wake deficit is modeled with an initial wake deficit at the rotor disk with tip and root losses depending on the energy extraction. In order to get the initial deficit, the energy extraction is mapped by applying Prandtl's root and tip loss function Γ_{Prandtl}. Applying the energy conservation assumption yields

$$(v_0 + s\Gamma_{\text{Prandtl}})^2 - (1 - c_P)v_0 = 0,$$ (5)

with the power coefficient c_p. Solving this equation for s gives the initial wake deficit

$$\Psi_{\text{init}} = s_{\text{solution}}\Gamma_{\text{Prandtl}}.$$ (6)

An exemplary initial wake deficit Ψ_{init} is shown in Figure 5.

The wake is evolving as it moves away from the wind turbine. New energy is flowing from the side and above and the flow is mixed. Physically these dynamics are described via the Navier-Stokes equations. These are partial differential equations and it would be a very complex task to estimate the wake using these equations. However, here an empirical model is used which models the wake recovery. In contrast to other wake models, however, the wake evolution is modeled by a Gaussian shape 2D filter. The 2D filter Ξ depends on the distance d behind the wind turbine

$$\Xi(d, y_i, z_i) = \exp\left(\frac{y_i^2 + z_i^2}{2\sigma_f^2(d)}\right)$$ (7)

with

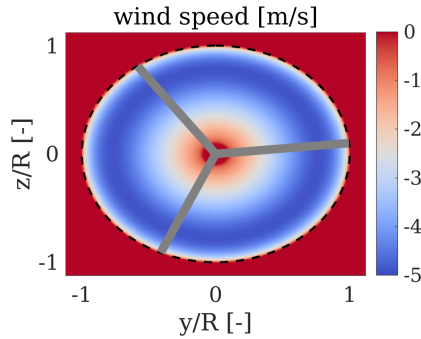$$\sigma_f(d) = \frac{d \cdot \epsilon}{2\sqrt{2\log(2)}}$$ (8)

7

Figure 5. The initial wake deficit directly evaluated at the rotor (at $0\,\mathrm{m}$ downstream). The mean hub-height wind speed $(8\,\mathrm{ms^{-1}})$ was removed for simplicity. No yaw misalignment is applied.

and y_i and z_i the grid points in distance d. With the parameter ϵ the dissipation rate can be set.

Thus, for every distance behind the rotor, the wake can be evaluated using the initial wake deficit Ψ_{init} and the filter (7). The wake deficit results from the convolution of the initial wake deficit Ψ_{init} with the filter $\Xi(d, y_i, z_i)$ to

$$\Psi(d, y_i, z_i) = \Xi(d, y_i, z_i) * \Psi_{\mathrm{init}} \tag{9}$$

5 **4.1.2   Wake deflection model.**

The wake deflection caused by a yaw misalignment γ is additionally modeled. The relationship is derived in the study of Jiménez et al. (2010) and was successfully used in an optimization of the yaw angles for a wind farm in Gebraad et al. (2014). The angle of the wake with respect to the main wind direction is

$$\xi(d, c_T, \gamma) = \frac{\xi_{\mathrm{init}}(c_T, \gamma)}{\left(1 + \beta \frac{d}{D}\right)^2}, \tag{10}$$

10 with the initial angle of the wake at the rotor

$$\xi_{\mathrm{init}}(c_T, \gamma) = \frac{1}{2} \cos^2(\gamma) \sin(\gamma) c_T \tag{11}$$

and model parameter β, which defines the sensitivity of the wake deflection to yaw and is here assumed to be known in advance. Further, c_T is the thrust coefficient and D the rotor diameter. Further, the yaw induced deflection at the downwind position d is according to Gebraad et al. (2014)

15 $$\delta_{\mathrm{yaw}}(d, c_T, \gamma) = -\xi_{\mathrm{init}}(c_T, \gamma) \frac{D}{30\beta} \left[15 \left(1 - \frac{1}{1 + \frac{2\beta d}{D}} \right) + \xi_{\mathrm{init}}(c_T, \gamma)^2 \left(1 - \frac{1}{\left(1 + \frac{2\beta d}{D}\right)^5} \right) \right]. \tag{12}$$

The rotation is applied to the wake deficit and yields a u and v component of the wake model,

$$\begin{bmatrix} \Psi_{u,i} \\ \Psi_{v,i} \\ 0 \end{bmatrix}_W = \begin{bmatrix} \cos\xi(d, c_T, \gamma) & -\sin\xi(d, c_T, \gamma) & 0 \\ \sin\xi(d, c_T, \gamma) & \cos\xi(d, c_T, \gamma) & 0 \\ 0 & 0 & 1 \end{bmatrix} \begin{bmatrix} \Psi_i \\ 0 \\ 0 \end{bmatrix}_W. \tag{13}$$

8

In Figure 6 two different wake situations are shown, the first is a non yawed case and in the second case the turbine is yawed with $\gamma = 25 \deg$. In both cases the underlying wind field has a mean hub-height free stream wind speed of $v_0 = 16\,\mathrm{m/s}$ and no vertical shear.
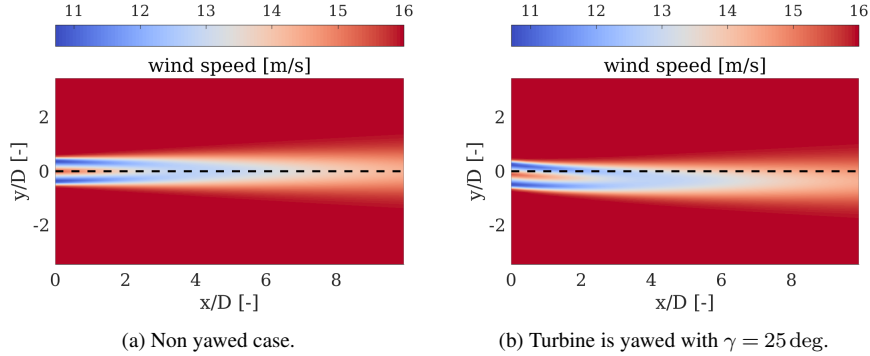

(a) Non yawed case.   (b) Turbine is yawed with $\gamma = 25 \deg$.

Figure 6. Visualization of two wake situations within a constant wind field of $v_0 = 16\,\mathrm{m/s}$, axial induction $a = 0.15$ and dissipation rate $\epsilon = 0.1$.

5   The estimation task - model-based wake tracking

5   As summarized before the estimation task performs the wake tracking using the presented wake model. To perform a lidar-based waked tracking a lidar model is needed. First, the lidar model is presented and then the wake tracking approach is described. Finally, estimation results of two different cases are presented and discussed.

5.1   Lidar model

The lidar measurements can be modeled by a point measurement in the wind field. In the inertial coordinate system this is done

10   by a projection of the wind vector $\begin{bmatrix} u_i & v_i & w_i \end{bmatrix}_I^T$ onto the normalized laser vector in the i-th point $\begin{bmatrix} x_i & y_i & z_i \end{bmatrix}_I^T$ with focus distance $f_i = \sqrt{x_{i,I}^2 + y_{i,I}^2 + z_{i,I}^2}$ by

$$v_{los,i} = \frac{x_{i,I}}{f_i} u_{i,I} + \frac{y_{i,I}}{f_i} v_{i,I} + \frac{z_{i,I}}{f_i} w_{i,I}. \tag{14}$$

5.2   Model-based wake tracking

As depicted in Figure 3 the model based wind field reconstruction method estimates the model parameter by minimizing the

15   error between measured line-of-sight wind speed $v_{los,m}$ and simulated line-of-sight wind speed $v_{los,s}$. A nonlinear optimization

problem is formed for n measurement points. This yields

$$\min_p f(x) = \min_p \begin{bmatrix} (v_{los,m,1} - v_{los,s,1})^2 \\ \vdots \\ (v_{los,m,n} - v_{los,s,n})^2 \end{bmatrix}, \tag{15}$$

where in p all free model parameters are included. The free model parameters are listed in Table 1. An example of an estimation step of the wake tracking from a measurement campaign at the alpha ventus offshore wind farm is shown in Figure 7.
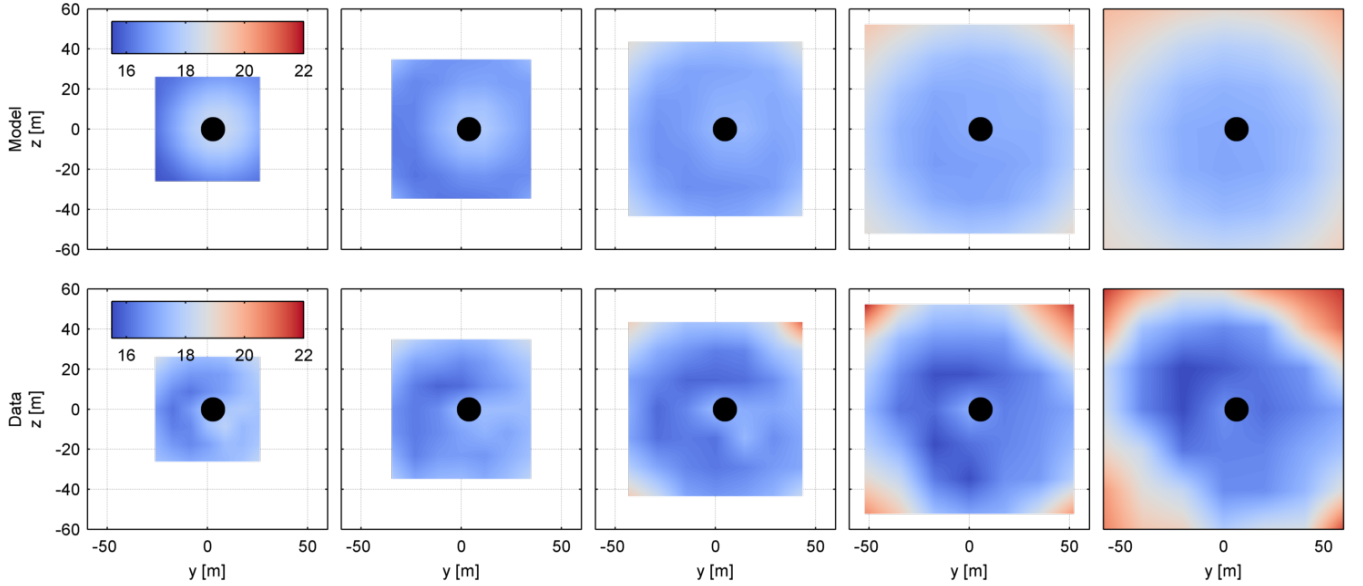

Figure 7. An exemplary estimation step of the wake tracking. The simulated lidar measurements in the first row are compared to the measured lidar data in the second row for five downstream distances from 0.6 to 1.4 times the rotor diameter (from left to right, looking downstream). The estimated wake center is marked with the black dot.

Table 1. The free model parameter for the wind field model which are estimated in the optimizer.

underlaying wind field		wake model	
v_0	rotor effective wind speed	c_T	thrust coefficient
δ_V	vertical linear shear	c_P	power coefficient
		γ	turbine yaw angle
		ϵ	wake dissipation coefficient

5.3 Evaluation and discussion

Figure 7 shows that the model fits well for the application and can be applied with real measurement data. In the following, SOWFA (Churchfield and Lee (2012)) is considered as simulation tool. Flow snapshots of a simulation of a single wind turbine are stored. The flow field is then scanned with a lidar simulator. The lidar scans with a 7×7 grid at five distances from 0.6 to 1.4 times the rotor diameter ($D = 126\,\mathrm{m}$). Two different cases are analyzed: First, a case where the turbine is aligned with the wind direction. The estimation results are shown in Figure 8. Second, the turbine is misaligned to deflect the wake. The results of the wake tracking is shown in Figure 9. In both figures the wake center is estimated at the furthest scanning distance of $1.4D = 176.4\,\mathrm{m}$. In both cases the method shows the ability of estimating the wake parameter and tracking the wake center.

As mentioned before the wake center position needs to be calculated using a specific definition and there is no direct measurable representation of it. In Figure 10 the lidar-based wake tracking is compared to the wake center estimation using the definition of Eq. (1) without any filtering.

6 The control task

The following closed-loop controller was first presented in Raach et al. (2016) and is recapped here.

As mentioned above, the reaction of the wake to a yaw action can only be measured with a time delay. To control a delayed system, the Smith Predictor approach has been derived and used in many applications. Internal model control is the basic idea of a Smith Predictor.

The presented controller follows the idea of internal model control in which the difference between the actual system output and a predicted output is used within the controller to regulate the system. Therefore, a model is necessary for describing the wake effects in a simplified but sufficient way. It consists of the controller which is a classical proportional-integral controller. Further, an internal model is used which approximates the real system behavior. The wake propagation which exists because the wake flow has to evolve until it reaches the measurement location of the lidar system is approximated with a delay. The time delay τ varies with respect to the mean wind speed. Finally, a filter is needed to cancel out controller actions which can not be observed because of the time difference between control action and measurement location. Figure 11 shows the general concept of the controller.

6.1 Internal wake model of the controller

As depicted in Fig. 11, the wake controller needs an internal model to predict the reaction of the wake to the demanded yaw angle. The internal wake model includes the yaw actuator and the yaw induces wake deflection. For the wake model the assumptions of a constant thrust coefficient is made. Altogether, this yields an internal controller model $\widetilde{\Psi}$ of the reality Ψ:

$$\widetilde{\Psi} : \begin{cases} \ddot{\gamma} + 2d\omega\dot{\gamma} + \omega^2\gamma = \omega^2\gamma_{dem} & \text{yaw actuator dynamic} \\ \tilde{y} = \delta_{\mathrm{yaw}}(d_{\mathrm{Lidar}}, c_{T,\mathrm{const}}, \gamma) & \text{wake deflection model} \end{cases} \tag{16}$$

with γ_{dem} the demanded yaw angle and d_{Lidar} the distance to the measurement location.
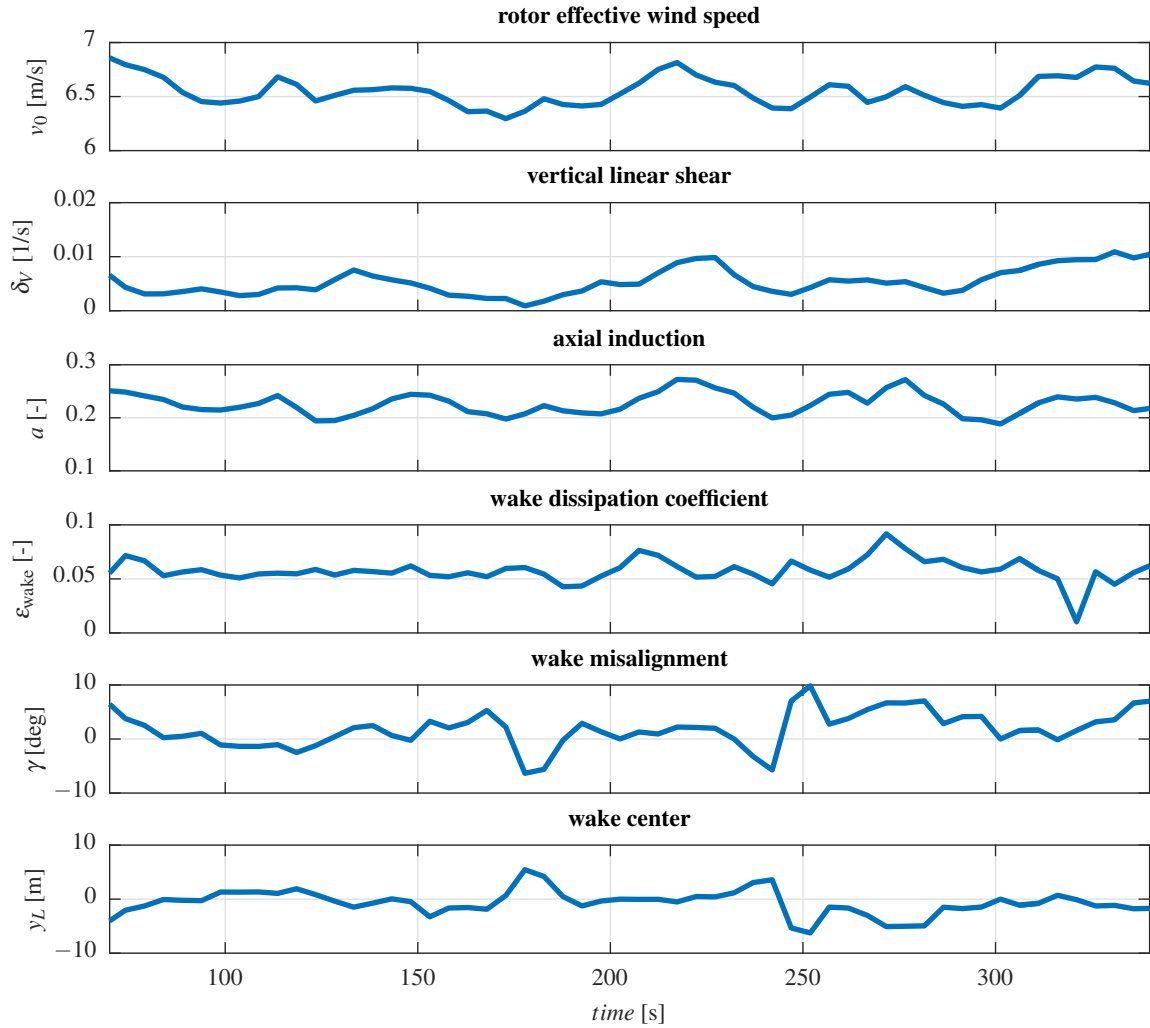
Figure 8. Time results of the wake tracking of a SOWFA simulation. The wind turbine is aligned with the main wind direction. The lidar scanned in a 7×7 grid at five distances from $0.6D$ to $1.4D$. The wake center is estimated at the furthest scanning distance $1.4D = 176.4\,\mathrm{m}$
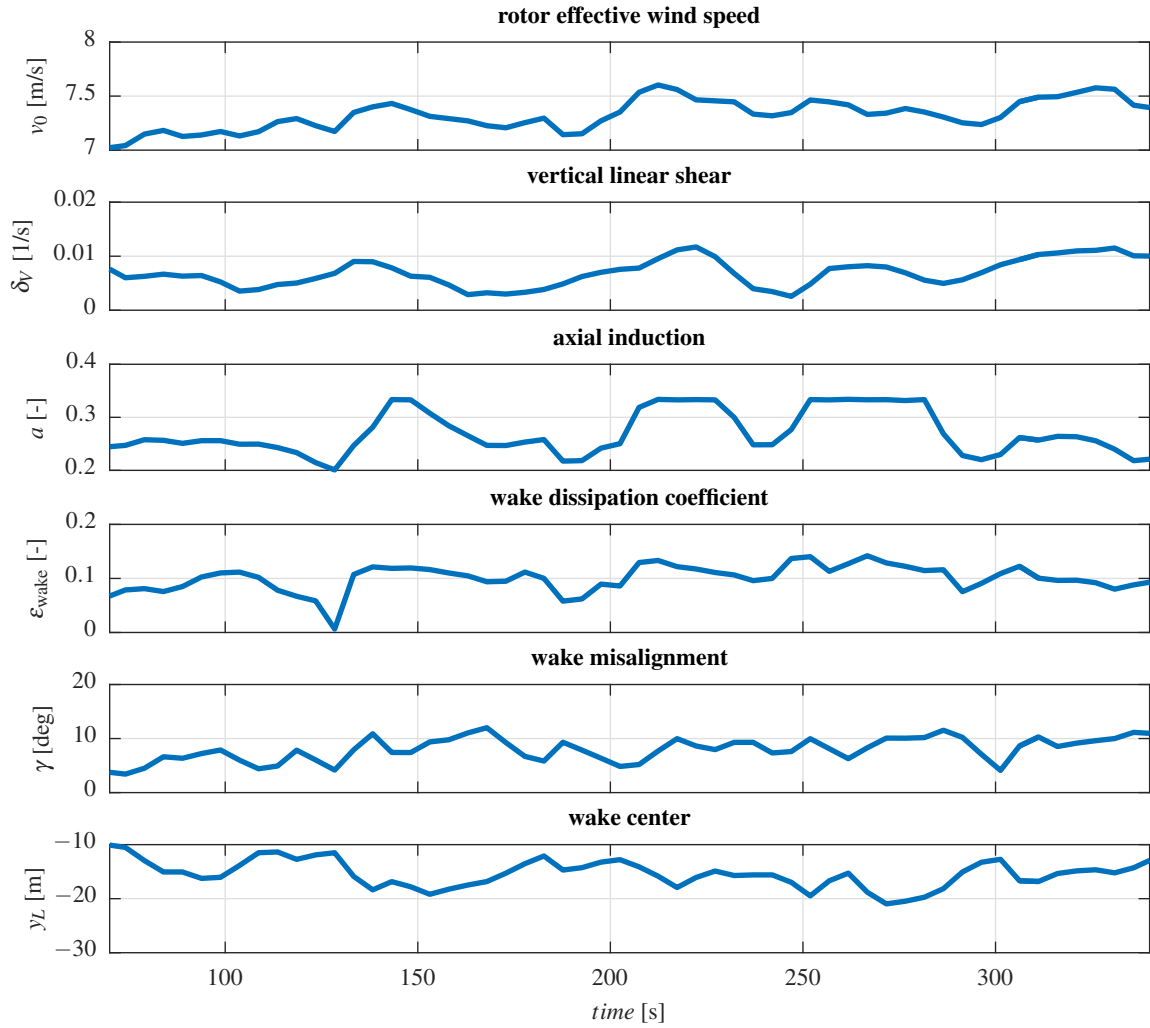
Figure 9. A second time evolution of the different estimated wind field and wake quantities. In this case, the wind turbine is misaligned and the wake is deflected. The lidar scanned in a 7×7 grid at five distances from $0.6D$ to $1.4D$. The wake center is estimated at the furthest scanning distance $1.4D = 176.4\,\mathrm{m}$
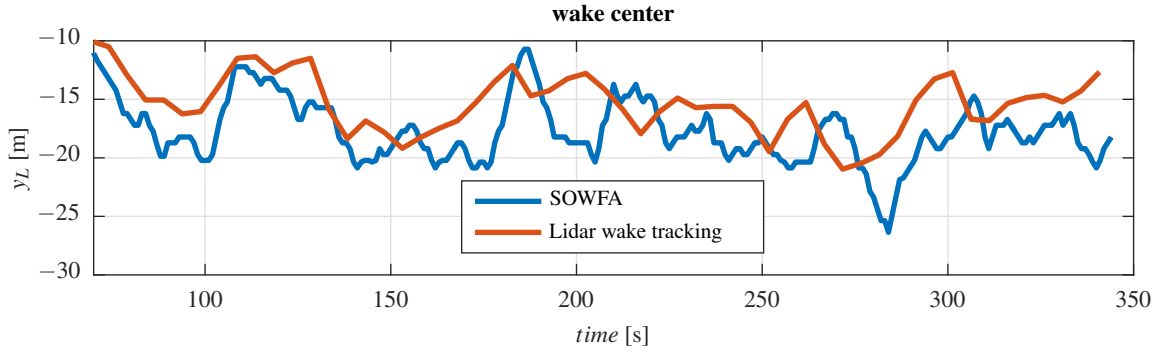
Figure 10. Comparison between the wake center estimation (see Eq. (1)) and the lidar-based wake tracking method.
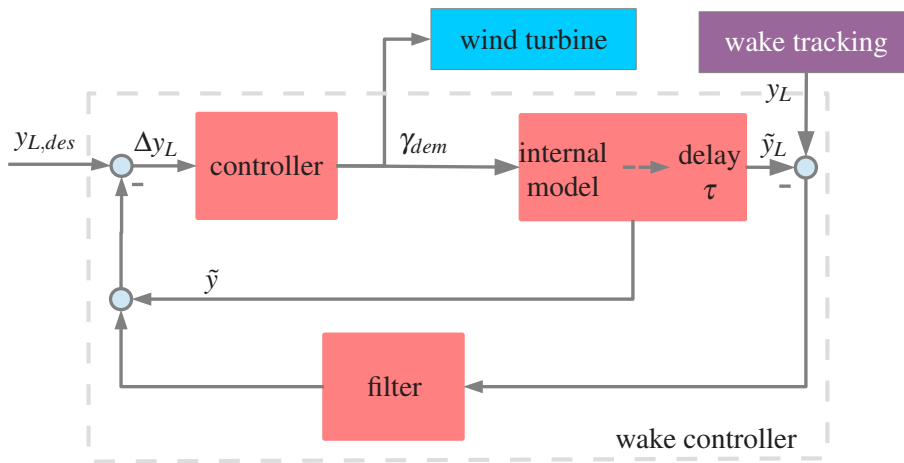

Figure 11. The general structure of the wake steering controller: The controller, a simplified wake model and the wake propagation modeled with a delay, and the filter. The controller uses the difference, δy_L, between the predicted output $\tilde{y}$, the measured output y_L and the desired output $y_{L,des}$ to set the demanded yaw angle γ_{dem}.

There is a time delay because the wake first needs to evolve to the measurement location:

$$\tilde{y}_L(t) = \tilde{y}(t - \tau). \tag{17}$$

For the controller design, the time delay is approximated using the Padé approximation of time delays, see Skogestad and Postlethwaite (2005).

5 **6.2 Controller design**

The primal goal of the wake controller is to steer the wake center to a desired point in a defined distance by yawing the wind turbine. As mentioned, this is done using a Smith Predictor, which uses an internal model to predict the output reaction. Then

14

the predicted wake center position and the filtered error between predicted and measured wake center position is fed back to the controller.

6.2.1 Controller

A standard proportional-integral (PI) controller is used. It is designed such that the closed-loop performance with the internal model (16) meets a phase margin of $60\,\mathrm{deg}$ and a closed-loop bandwidth of $\omega_{\mathrm{CL}} = \frac{1}{2\tau}$. This yields a controller of the form

$$u = K_p\Big(\Delta y_L + \frac{1}{T_i}\int \Delta y_L \mathrm{d}t\Big), \tag{18}$$

with the proportional gain K_p and the time constant T_i.

6.2.2 Filter

The wake propagation and the caused delay disables a direct measure of a yaw change and because of that one has to filter the measured feedback to prevent non-observable yaw actions. Since the delay τ is time varying and depends on the mean wind speed the filter has to be adaptable. Therefore, the cutoff frequency of the butterworth low-pass filter is set to $\omega_{\mathrm{filter}} = \frac{\pi}{8\tau}$.

6.3 Evaluation and discussion

In the following the wake controller is analyzed. Further, the sensitivity and the complementary sensitivity of the closed-loop system is assessed. Consider Skogestad and Postlethwaite (2005) for a detailed description on controller design and analysis.

6.3.1 Controller analysis

In the following the transfer function of the wake controller is assessed. As shown in Figure 11 the wake controller consists of the internal controller C, an internal model $\widetilde{\Psi}$, the time delay approximation W and the filter F. Having merged all parts the wake controller K is

$$K = \frac{F}{(1 + C\,\Psi\,(1 - F\,W))}. \tag{19}$$

Figure 12 shows the bode analysis of the wake controller K. The controller shows integration behavior, starting with $-90\,\mathrm{deg}$ phase.

6.3.2 Closed-loop analysis

To perform closed-loop analysis the internal controller model $\widetilde{\Psi}$ is transformed to Laplacian space yielding the plant G. Then, the sensitivity S and the complementary sensitivity T that are

$$S = \frac{1}{1 + GK} \tag{20}$$

$$T = \frac{GK}{1 + GK}, \tag{21}$$

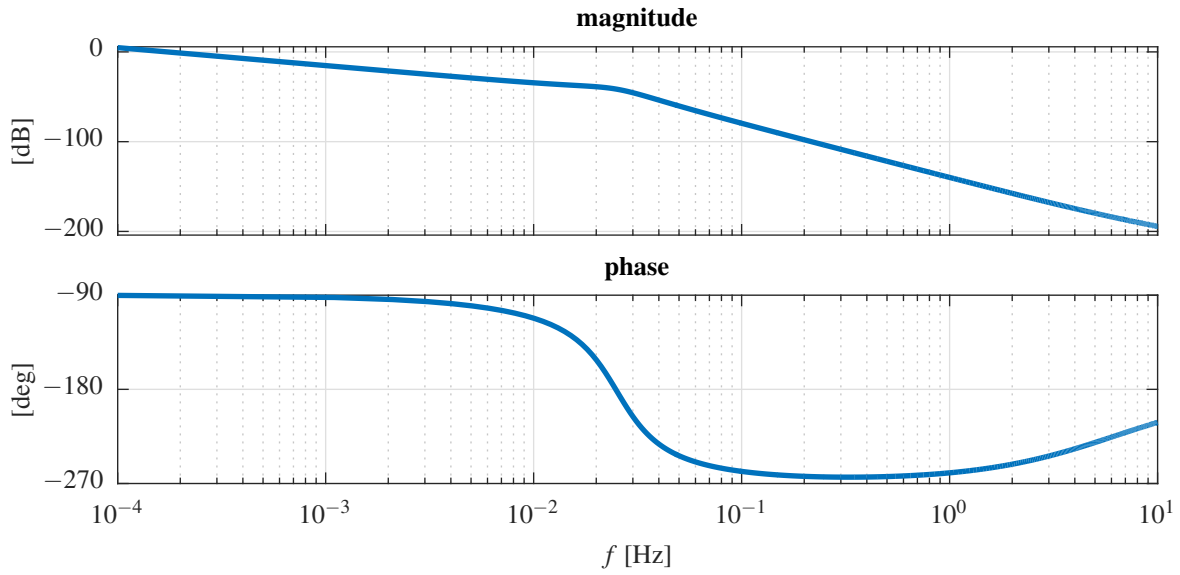with the controller K are assessed and shown in Figure 13.

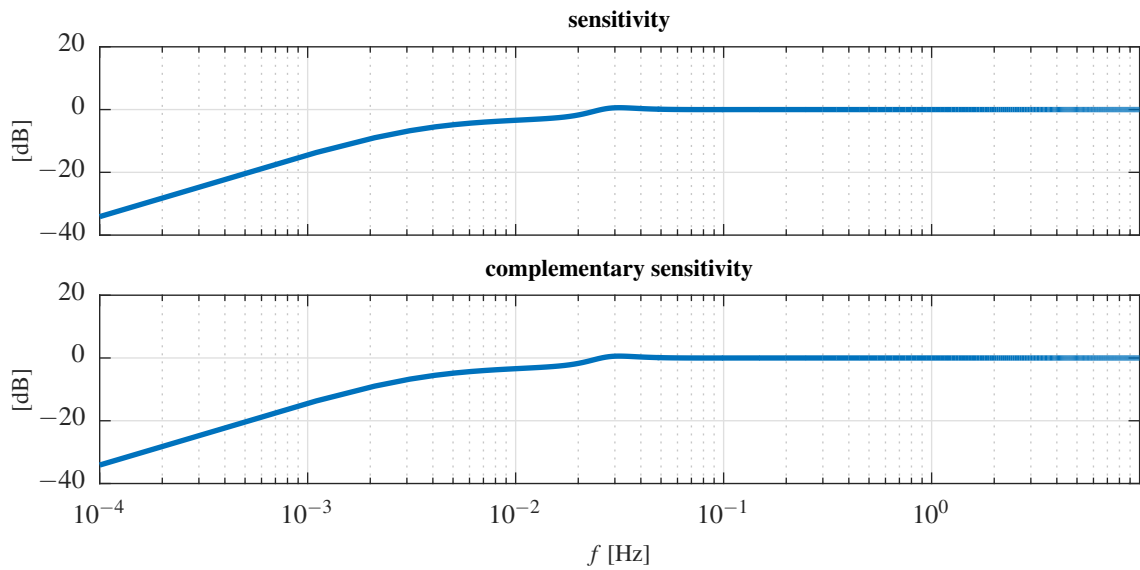**Figure 12.** Bode analysis of the designed controller K.

Figure 13. Sensitivity S and complementary sensitivity T analysis of the closed-loop system.

7 Conclusions

This paper introduces first a method which uses lidar measurements to estimate wind field parameters and enables a tracking of the wake center position. Second, a controller is presented which uses this information to redirect the wake to a desired position. In two different cases using simulated lidar measurements of SOWFA simulations, the wake tracking shows promising results in estimating the wake center. The difficulty in wake center position definition is elaborated. A definition is used and the wake tracking results are compared to it. The challenges of a lidar-based wake redirecting control problem are discussed and an appropriate controller is designed to meet the desired requirements. This enables the next step towards a closed-loop wake redirecting in a high fidelity simulation tool which is aimed as a next step.

As an outlook, the presented framework of lidar-based closed-loop wake steering offers new possibilities for wind farm control. In a next step, it will be implemented and tested in a high fidelity simulation tool and tested in real time. For the control problem, different controller approaches will be investigated such as $\mathcal{H}_\infty$ controllers or robust controllers. Dynamic estimation techniques as well as other wake estimation models will be used for comparing the ability of tracking the wake and finding the most suitable approach for this task.

References

Boersma, S., Doekemeijer, B., Gebraad, P., Fleming, P.and Annoni, J., Scholbrock, A., Frederik, J., and van Wingerden, J.-W.: A Tutorial on Control-Oriented Modeling and Control of Wind Farms, in: Proceedings of the American Control Conference (ACC), 2017.

Borisade, F., Luhmann, B., Raach, S., and Cheng, P. W.: Shadow Effects in an Offshore Wind Farm - Potential of Vortex Methods for Wake Modelling, in: Proceedings of the German Wind Energy Conference DEWEK, Bremen, Germany, 2015.

Churchfield, M. and Lee, S.: NWTC design codes-SOWFA, URL: http://wind. nrel. gov/designcodes/simulator s/SOWFA, 2012.

Fleming, P., Gebraad, P. M., Lee, S., Wingerden, J.-W., Johnson, K., Churchfield, M., Michalakes, J., Spalart, P., and Moriarty, P.: Simulation comparison of wake mitigation control strategies for a two-turbine case, Wind Energy, 18, 2135–2143, 2014a.

Fleming, P. A., Gebraad, P. M., Lee, S., van Wingerden, J.-W., Johnson, K., Churchfield, M., Michalakes, J., Spalart, P., and Moriarty, P.: Evaluating techniques for redirecting turbine wakes using SOWFA, Renewable Energy, 70, 211–218, 2014b.

Gebraad, P. M. O., Teeuwisse, F. W., van Wingerden, J., Fleming, P., Ruben, S. D., Marden, J. R., and Pao, L. Y.: Wind plant power optimization through yaw control using a parametric model for wake effects—a CFD simulation study, Wind Energy, 19, 95–114, doi:10.1822/we, 2014.

Jiménez, Á., Crespo, A., and Migoya, E.: Application of a LES technique to characterize the wake deflection of a wind turbine in yaw, Wind Energy, 13, 559–572, 2010.

Raach, S., Schlipf, D., Haizmann, F., and Cheng, P. W.: Three Dimensional Dynamic Model Based Wind Field Reconstruction from LiDAR Data, in: Journal of Physics: Conference Series: The Science of Making Torque From Wind, vol. 524, Copenhagen, Denmark, 2014.

Raach, S., Schlipf, D., Borisade, F., and Cheng, P. W.: Wake redirecting using feedback control to improve the power output of wind farms, in: Proceedings of the American Control Conference (ACC), Boston, USA, 2016.

Schlipf, D., Rettenmeier, A., Haizmann, F., Hofsäß, M., Courtney, M., and Cheng, P. W.: Model Based Wind Vector Field Reconstruction from Lidar Data, in: Proceedings of the German Wind Energy Conference DEWEK, Bremen, Germany, 2012.

Skogestad, S. and Postlethwaite, I.: Multivariable Feedback Control: Analysis and Design, John Wiley & Sons, 2005.

Vollmer, L., Steinfeld, G., Heinemann, D., and Kühn, M.: Estimating the wake deflection downstream of a wind turbine in different atmospheric stabilities: an LES study, Wind Energy Science, 1, 129–141, doi:10.5194/wes-1-129-2016, 2016.